JOURNAL OF CATALYSIS 93, 409–416 (1985)

Kinetic Studies with a Sulfur-Tolerant Methanation Catalyst[1]

PEGGY Y. HOU AND HENRY WISE

Solid State Catalysis Laboratory, SRI International, Menlo Park, California 94025 and Department of Materials Science and Engineering, Stanford University, Stanford, California 94305

Received May 25, 1984; revised December 12, 1984

The kinetics of methane formation by the molybdenum disulfide-catalyzed reaction of hydrogen and carbon monoxide are examined. The stoichiometry of the reaction is found to be given by

$$2CO + 2H_2 \rightarrow CH_4 + CO_2.$$

The reaction rate is of first order in carbon monoxide and of half order in hydrogen. Carbon dioxide, one of the reaction products, causes some inhibition in methanation rate. The activation energy for the molybdenum disulfide-catalyzed reaction is 31 kJ mol^{-1}, considerably less than observed for transition-metal catalyzed methanation. The thermodynamic sulfur activity of the catalyst influences the reaction kinetics by governing the defect structure of molybdenum disulfide. High S/Mo ratios in the solid phase enhance the dissociative chemisorption of hydrogen. © 1985 Academic Press, Inc.

INTRODUCTION

In the conversion of syngas (CO and H_2) to hydrocarbon fuels, a number of transition-metal catalysts have been used, including nickel, iron, cobalt, and ruthenium (*1*). However, these metals impose certain operating limitations because of their susceptibility to deactivation by surface carbon and poisoning by surface sulfur (*2*). Thus, in the case of coal-derived syngas, the H_2/CO ratio has to be adjusted to values greater than two by water-gas shift, and the sulfur impurities have to be removed to very low levels (less than 0.05 ppm) from the feed stream. In addition, the hydrocarbon synthesis is very hydrogen intensive since some of the hydrogen used is converted to water in the product stream, as exemplified by the following overall stoichiometries for paraffinic and olefinic hydrocarbons:

$$(2n + 1)H_2 + nCO \rightarrow C_nH_{2n+2} + nH_2O$$

$$2nH_2 + nCO \rightarrow C_nH_{2n} + nH_2O$$

In view of these considerations we have examined the catalytic properties for methanation of a nonmetal catalyst, molybdenum disulfide. Its catalytic properties for hydrocarbon synthesis have been reported and its insensitivity to sulfur poisoning recognized (*3–8*). However, the reaction kinetics for methane formation and the influence of hydrogen sulfide on the reaction mechanism and the defect structure of the catalyst have not been evaluated. The objectives of our research were a detailed investigation of the methanation kinetics and the influence of the solid-state properties of the catalyst on catalytic activity. Of special interest was the entirely different reaction stoichiometry for methanation favored by molybdenum sulfide as compared to the transition metals. In the case of molybdenum sulfide the overall synthesis reaction leading to methane is

$$2CO + 2H_2 \rightarrow CH_4 + CO_2$$

In this case the stoichiometric H_2/CO ratio is unity. Thus all the hydrogen consumed is incorporated into methane. Also the absence of water as a product limits the contribution of the water-gas shift reaction for which the molybdenum sulfide exhibits significant activity (*9*).

[1] Support of this work by the Gas Research Institute is gratefully acknowledged.

0021-9517/85 $3.00
Copyright © 1985 by Academic Press, Inc.
All rights of reproduction in any form reserved.

EXPERIMENTAL DETAILS

1. Catalyst preparation. The catalyst used in this study was prepared (*9*) by impregnation to incipient wetness of a high-surface-area alumina support (γ-alumina, 320 m^2/g) with an aqueous ammoniacal solution of ammonium heptamolybdate. Its concentration was adjusted to yield the desired weight loading of molybdenum (10 wt%). The catalyst sample was dried in a vacuum oven at 350 K, and calcined in flowing oxygen at 1 atm and 773 K. Pretreatment of the catalyst involved exposure at elevated temperatures to gas mixtures of H_2S, H_2, and He of various compositions for a period of 12 to 17 h. The H_2S/H_2 ratio was varied over a range of compositions in order to vary the thermodynamic sulfur activity in the solid phase and thereby its defect structure.

2. Reactant gases. The reactants included hydrogen (purified by diffusion through a Pd–Ag thimble), and carbon monoxide (99.99 vol% purity) stored in aluminum cylinders and freed of metal carbonyls by passage through a molecular-sieve trap cooled by dry ice–acetone. The H_2S level in the feed gas was adjusted to the desired level by dilution of a gas mixture of 5 vol% H_2S in He contained in aluminum cylinders.

3. Catalytic measurements. A continuous-flow cylindrical microreactor made of quartz was used for the kinetic studies. The reactor was heated by an external cylindrical furnace, whose temperature was monitored by an external thermocouple, and maintained at the desired level by an automatic temperature controller.

In addition, a small recirculating reactor was employed for detailed kinetic studies of the effect of reaction products on the methanation rate. The catalyst sample (0.5 to 1 g) was placed on a fritted quartz disk located inside the reactor. Aliquots of the feed and product gas could be diverted to a sampling loop and subjected to quantitative chemical analysis by gas chromatography for CO, CO_2, CH_4, H_2, and H_2O.

The GC column contained "Spherocarb" (80–100 mesh) and operated at 315 K. In addition, gas aliquots were analyzed quantitatively for sulfur-containing species (H_2S, COS, CS_2) by passage through a "Chromosil/310" column at 315 K and detected by means of a flame photometric analyzer (*11*). The entire sampling system was wrapped with heating tape and heated to about 325 K to prevent condensation of any product, such as hydrocarbons up to C_5.

4. Adsorption studies. To characterize the adsorption characteristics of the catalyst under study we employed a microreactor in which the catalyst sample was pretreated first at elevated temperatures (>750 K) with H_2S–H_2 gas mixtures of the desired composition for periods in excess of 10 h. Then the gas stream was switched to argon and the temperature raised to 875 K for 1 to 2 h preceding the adsorption studies. Subsequently, the sample was cooled to 373 K in flowing argon. The adsorptive capacity of the sample was determined by exposure to pulses of the gas under study, until no further pickup of the gas was detectable in the calibrated thermal conductivity cell connected to the outlet of the reactor. The amount of gas adsorbed from each pulse was evaluated from the difference between the inlet and outlet concentrations.

EXPERIMENTAL RESULTS

1. Sulfidation of Catalyst

In the oxide form the MoO_3/Al_2O_3 catalyst exhibits no methanation activity. However, after reductive sulfidation to molybdenum disulfide the synthesis of methane from syngas is observed. As noted already in an earlier publication (*9*), the ratio of S/Mo in the sulfided catalyst has a profound effect on its catalytic properties. Thus the process of reductive sulfidation of the MoO_3/Al_2O_3 catalyst was followed in some detail. In terms of an overall stoichiometry the reaction may be written as

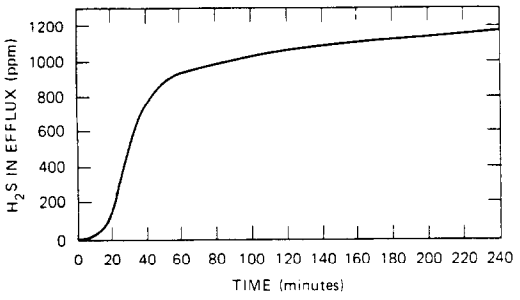

FIG. 1. Sulfur uptake by catalyst at 723 K (H_2S/H_2 = 1300 ppm; space velocity = 2.3×10^4 hr^{-1}).

$$MoO_3 + 2H_2S + H_2 \rightarrow MoS_2 + 3H_2O \quad (1)$$

involving the conversion of Mo(VI) oxide to Mo(IV) sulfide. The molybdenum–sulfide phase exhibits a wide range of sulfur-to-molybdenum ratios. Its equilibrium composition ($Mo_{1+x}S_2$) is governed by thermodynamic activity of sulfur in the gas phase. In our experiments we adjusted the sulfur activity by varying the H_2S/H_2 ratio at the reactor inlet. The uptake of sulfur by the catalyst and the attainment of the solid–gas equilibrium was monitored by measuring the H_2S level in the reactor efflux.

A typical experimental curve depicting the sulfidation process of the variation in H_2S level with a sample of MoO_3/Al_2O_3 is shown in Fig. 1. Initially all the H_2S is taken

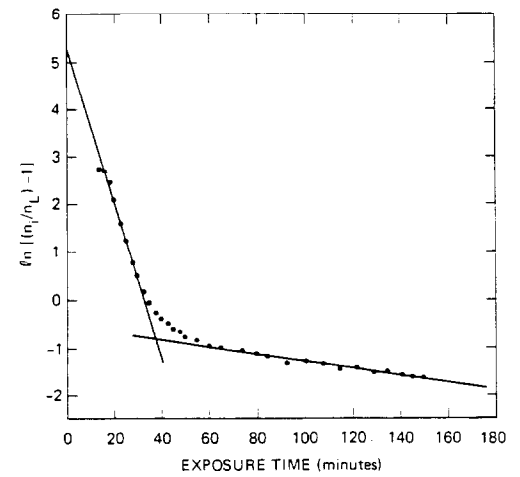

FIG. 2. Sulfidation kinetics at 723 K (H_2S/H_2 = 1300 ppm; space velocity = 2.3×10^4 hr^{-1}).

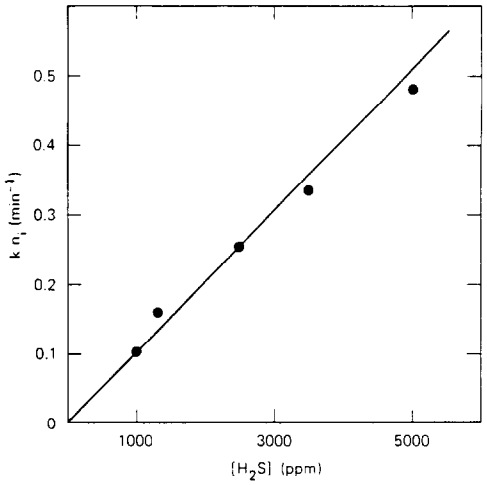

FIG. 3. Sulfidation rate at various sulfur activities (space velocity = 2.3×10^4 hr^{-1}; temperature = 723 K).

up by the sample. However, even after 4 h of exposure, incorporation of sulfur into the solid phase continues. We have analyzed the data in terms of a dynamic model with progressive first order layer-by-layer sulfidation process. Based on such a wavefront analysis (*10*) one finds that the process of sulfur pickup involves two steps, each occurring at different rates as manifested by the magnitude of two-line segments with dissimilar slopes (Fig. 2).

The rate of sulfur uptake during the first segment of sulfidation was found to be proportional to the concentration of H_2S in the feed stream (Fig. 3). The rate constants calculated for this process are summarized in Table 1. On the other hand, for the second segment of sulfur incorporation the rate was nearly independent of H_2S concentration, indicative of a diffusion-limited process.

For the different sulfur activities examined (Table 1) the sulfur uptake at the crossing point of the two-line segments correspond to S/Mo ~ 1.0. It indicates the incorporation of one sulfur atom per molybdenum atom and suggests the formation of molybdenum oxysulfide (MoO_2S or MoOS) as an intermediate in the reductive sulfidation of MoO_3. Also, the kinetic measure-

TABLE 1

Sulfidation Rate Constant at 723 K and Various Sulfur Activities[a]

$[H_2S/H_2]$ (ppm)	Rate constant, k (ppm^{-1} min^{-1}) × 10^4
1000	1.1
1300	1.3
2500	1.0
3500	1.0
5000	0.9
Average	1.1 ± 0.1

[a] Space velocity = 2.3×10^4 h^{-1}.

ments indicate that the formation of the oxysulfide proceeds more rapidly than the conversion to molybdenum disulfide. Apparently MoO_2 is not an intermediate state. Indeed, the sulfidation of MoO_2 to MoS_2 is a much slower process than the reductive sulfidation of MoO_3 to MoS_2 (*11–13*).

2. Methanation Kinetics

(*a*) *Effect of H_2S in feed gas.* Having established the exposure required to convert molybdenum trioxide to molybdenum disulfide, we examined the rate of methane formation as a function of the thermodynamic sulfur activity. An increase in H_2S/H_2 at constant equimolar syngas composition was accompanied by a significant rise in the methanation rate (Fig. 4). In these measurements the catalyst sample was converted to molybdenum sulfide in a flow-through reactor at 800 K for 18 to 25 h with a gas mixture containing H_2S and H_2 of the same composition as used subsequently in the methanation experiment. These studies were carried out under differential-reactor condition, i.e., <10% conversion. The pronounced variation in the methanation rate (Fig. 4) is associated with changes in the stoichiometry of the catalyst. Also the results indicate that MoO_3/Al_2O_3 does not exhibit any measurable methanation activity.

(*b*) *Orders of reaction.* The kinetic data on reaction order with respect to each of the reactants (H_2 and CO) was obtained by making up a three-component gas mixture containing hydrogen, carbon monoxide, and helium (diluent) and varying the concentration of one of the reactants in the feed gas while keeping the other constant. Again the total conversion of reactants was kept at less than 10 vol% so that we were operating in the differential reactor mode. By this means the reaction rate for methane formation was found to be of 0.5 order with respect to hydrogen (Fig. 5), and of first order with respect to carbon monoxide (Fig. 6).

Since carbon dioxide is a reaction product, its effect on the methanation rate was determined by addition of known concentrations of CO_2 to the three-component feed gas entering the differential reactor. The

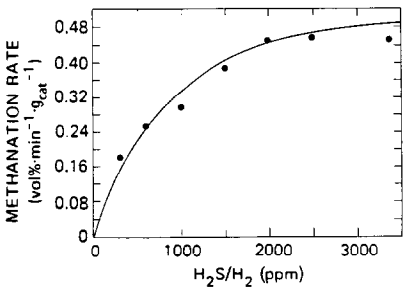

FIG. 4. Methanation rate at different H_2S levels in syngas (H_2 = CO = 20 vol%; He = 60 vol%; 1 atm; 800 K).

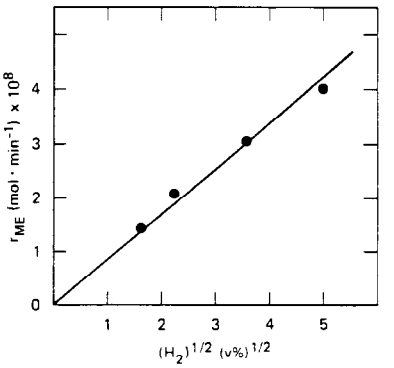

FIG. 5. Variation in methanation rate with hydrogen concentration at 723 K (total pressure = 1 atm; CO = 25 vol%; He diluent; H_2S = 10^4 ppm; space velocity = 2000 hr^{-1}).

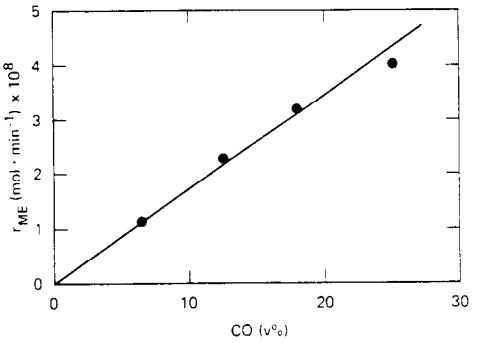

FIG. 6. Variation in methanation rate with carbon monoxide concentration at 723 K (total pressure = 1 atm; H_2 = 25 vol%; He diluent; H_2S = 10^4 ppm; space velocity = 2000 hr^{-1}).

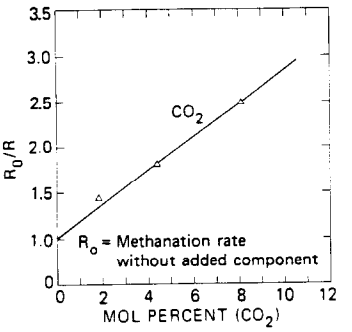

FIG. 7. Reciprocal methanation rate as a function of carbon dioxide concentration (37.5 vol% H_2, 37.5 vol% CO, 25 vol% He; 2500 ppm H_2S; 1 atm; 800 K).

results demonstrated a significant inhibition in methanation rate caused by carbon dioxide. The magnitude of this effect is apparent from the data in Fig. 7, in which the reciprocal of the methanation rate is plotted as a function of CO_2 added to the feed. Normalized to the rate without CO_2, a linear relationship is obtained between the reciprocal rate and the CO_2 concentration. The inhibitory effect by CO_2 produced during reaction becomes quite apparent during methanation in a recirculating reactor (Fig. 8). At more than 10 vol% conversion of CO, the methanation rate begins to decline relative to the initial rate.

DISCUSSION

The reaction kinetics derived from our experimental measurements indicate that the rate of methane formation is given by[2]

$$-\tfrac{1}{2}d(CO)/dt = d(CH_4)/dt = \frac{k_1(H_2S)^{1/2}(CO)(H_2)^{1/2}}{1 + \gamma(CO_2)} \quad (2)$$

and proceeds in accordance with the stoichiometric reaction

$$2CO + 2H_2 \rightarrow CH_4 + CO_2.$$

Thus we may write Eq. (2) to read

$$dx/dt = k_1'(a - x)(b - x)^{1/2}/(1 + \gamma x). \quad (3)$$

[2] The parentheses designate molar concentrations.

The term k_1' represents the product $[2k_1(H_2S)^{1/2}]$, with k_1 the rate constant. This grouping of terms is indicative of the fact that H_2S is not a reactant, but a term affecting the defect composition of the catalyst. The coefficient γ is associated with CO_2 inhibition of the methanation rate. The terms a and b represent the initial concentrations of carbon monoxide and hydrogen. For equimolar concentration of CO and H_2 ($a = b$) and at low conversion (<10 vol%), one obtains on integration of Eq. (3):

$$k_1't = 2\left[(1 + b\gamma)\left(\frac{1}{\sqrt{b - x}} - \frac{1}{\sqrt{b}}\right) - \gamma(\sqrt{b} - \sqrt{b - x})\right]. \quad (4)$$

To evaluate k_1' and γ the rate of methane consumption was measured in a fixed volume recirculating reactor over a range of temperatures. The composition of the re-

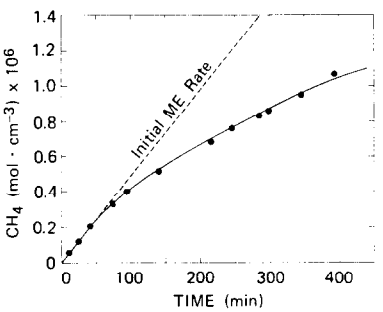

FIG. 8. Methane formation in recirculating reactor (800 K; 20 vol% H_2, 20 vol% CO, 60 vol% He; H_2S = 2500 ppm; pressure = 1 atm; 50 x 10^{-3} g catalyst).

acting gas mixture was monitored by withdrawal of small aliquots for chemical analysis of CH_4, CO_2, CO, and H_2 by gas chromatography.

At 800 K the rate constant was found to be $k_1' = 0.91\ min^{-1}$ which at 2500 ppm H_2S corresponds to $k_1 = 2.4 \times 10^7\ (mol\ cm^{-3})^{-1/2}\ min^{-1}$. For CO_2 inhibition one calculates an inhibition coefficient $\gamma = 0.65 \times 10^6\ (mol\ cm^{-3})^{-1}$. The rate data obtained at constant sulfur activity over a temperature range from 625 to 800 K permit evaluation of the activation energy for methanation. The data yield $E_a = 31.3 \pm 0.8\ kJ\ mol^{-1}$ (Fig. 9). It is quite apparent that this value is considerably smaller than for methanation catalyzed by nickel ($E_a \sim 100\ kJ\ mol^{-1}$).

The inhibition term γ is nonvariant over the temperature range studied. Mechanistically this term may originate from the propensity of the catalyst for water-gas shift (*9*). The reverse water-gas shift reaction ($CO_2 + H_2 \rightarrow CO + H_2O$) may be in competition with methanation. The details of this process remain to be elucidated.

Finally, the influence of the defect structure of the molybdenum–sulfide catalyst on methanation rate was examined. In previous studies (*14*) it had been demonstrated that the incorporation of sulfur in excess of the stoichiometric composition proceeds readily and yields a *p*-type semiconductor. For $Mo_{1-x}S_2$ (i.e., sulfur-rich molybdenum

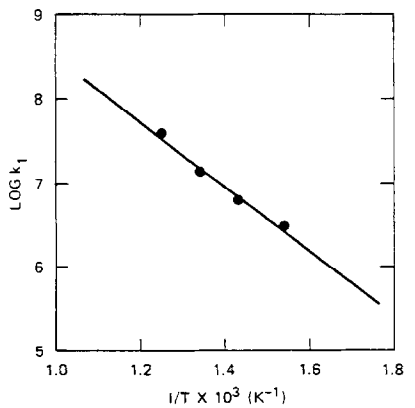

FIG. 9. Methanation rate constant at constant sulfur activity (2500 ppm H_2S in H_2).

sulfide) the addition of sulfur to the catalyst may be represented by the equilibrium (*14*).

$$H_2S \rightleftarrows H_2 + S^{2-} + 2p \qquad (5)$$

where p represents an electronic hole carrier and V_c a neutral cation vacancy. The equilibrium constant is given by

$$K = (H_2)(p^2)/(H_2S) \qquad (6)$$

and $(p) = [K(H_2S)/H_2)]^{1/2}$. Consequently the hole density of the catalyst is governed by the square root of the H_2S/H_2 ratio.

Since the methanation rate depends on $(H_2S/H_2)^{1/2}$ (Fig. 4), we conclude that during methanation the availability of holes and their interaction with a reactant are important. Most likely this process involves a hole acceptor such as hydrogen, which undergoes dissociative chemisorption by the reaction

$$H_2 + 2p \rightarrow 2H^+ \qquad (7)$$

The protonic species is bound to the cation vacancy. Similar conclusions were reached in our earlier studies of the HDS reaction catalyzed by single-crystal molybdenum sulfide (*14*). The hole density, as determined by electrical conductivity measurements with single-crystal molybdenum sulfide, was found to govern hydrogen chemisorption and thereby the HDS rate.

On the basis of such solid-state effects the chemisorption of hydrogen and carbon monoxide was examined as a function of sulfur activity. A series of measurements were carried out in which catalyst samples, after pretreatment in H_2S/H_2 (as described in Fig. 4), were exposed to pulses of H_2 (1 vol% in Ar) until saturation coverage was attained. Indeed the amount of hydrogen adsorbed varied with the square root of H_2S/H_2 during pretreatment (Fig. 10). This enhancement in the hydrogen chemisorption capacity appears to be responsible for the enhanced methanation activity. The hole carriers facilitate the dissociative adsorption of H_2 on the surface of the catalyst (reaction (7)).

As yet the mechanism of methanation

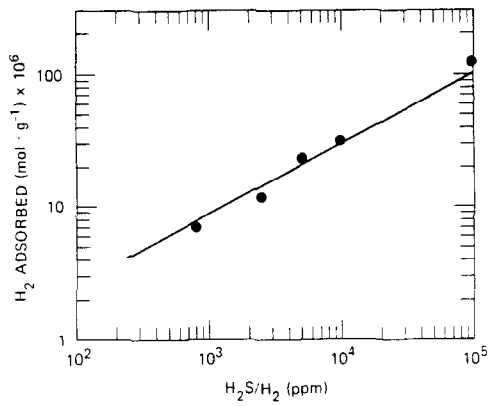

FIG. 10. Hydrogen adsorption capacity as a function of sulfur activity of catalyst.

catalyzed by molybdenum sulfide has not been established in detail. Dissociative chemisorption of hydrogen occurs. Adsorption of CO appears to involve an associative precursor state. However, the formation of CO_2 as a major product points to breakage of the carbon-to-oxygen bond during an early step in the methanation reaction.

To determine whether dissociation of CO occurs on Mo-based catalysts, we carried out an isotope-exchange study in which we measured the degree of scrambling on exposure of the catalyst to the two CO isotopes $C^{12}O^{18}$ and $C^{13}O^{16}$. The formation of $C^{12}O^{16}$ and $C^{13}O^{18}$ in the product stream is indicative of rupture of the C-to-O bond during the interaction of CO with the surface at elevated temperatures.

The experimental apparatus consisted of a quartz microreactor containing about 50 mg of the catalyst. Aliquots of mixed $C^{13}O^{16}$ and $C^{12}O^{18}$ gases were injected into the He carrier gas flowing continuously over the catalyst which had been pretreated at 723 K in 2500 ppm H_2S/H_2 for 12 h and subsequently cooled in He (freed of oxygen). The catalyst bed was heated with an external electrical furnace at a linear rate of 0.3 K s^{-1} to temperatures ranging from 375 to 775 K. The effluent gas composition was determined by continuously sampling with a quadrupole mass spectrometer analyzer. The concentrations of the four CO isotopes, $C^{12}O^{16}$, $C^{13}O^{16}$, $C^{12}O^{18}$, and $C^{13}O^{18}$, and two CO_2 isotopes, $C^{12}O_2^{16}$ and $C^{12}O^{16}O^{18}$, were analyzed simultaneously using an automatic peak selector.

The extent of isotope exchange, Φ, can be represented as

$$\Phi_{ij} = \frac{Y_{ij} - X_{ij}}{Z_{ij} - X_{ij}} \quad \begin{matrix} i = 12, 13 \text{ carbon isotope} \\ j = 16, 18 \text{ oxygen isotope} \end{matrix}$$

where

Φ_{ij} = the inlet fraction of the ij component

Y_{ij} = the outlet fraction of the ij component

X_{ij} = the inlet fraction of the ij component

Z_{ij} = the equilibrium fraction of the ij component.

The parameter Φ will vary from zero to one as the isotope distribution approaches equilibrium. Assuming a random distribution, we can define Z_{ij} as

$$Z_{ij} = (Y_{i16} + Y_{i18})(Y_{12j} + Y_{13j}),$$

i.e., the equilibrium fraction of the ij CO component is equal to the product of the outlet fraction containing the sum of the ith carbon isotopes multiplied by the outlet fraction containing the sum of the jth oxygen isotopes. For a random isotope distribution and in the absence of a kinetic isotope effect for exchange, we expect all Φ_{ij} values to be equal, $\Phi = \Phi_{ij}$, where Φ is the overall extent of exchange. Indeed, in our measurements, the four calculated Φ_{ij} for $C^{12}O^{16}$ (Φ_{11}), $C^{13}O^{16}$ (Φ_{21}), $C^{12}O^{18}$ (Φ_{12}), and $C^{13}O^{18}$ (Φ_{22}) agreed within experimental error for each dose of the $C^{13}O^{16}/C^{12}O^{18}$ mixture admitted to the presulfided catalyst. Figure 11 presents a plot of the parameter Φ versus temperature as obtained from a series of experiments. Isotope scrambling as a result of CO dissociation on the catalyst surface becomes significant at $T > 575$ K, a temperature considerably lower than used in the methanation studies. Based on the results presented, we conclude that the mechanism of methane synthesis involves

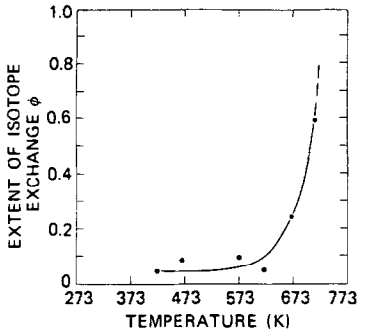

FIG. 11. CO isotope exchange.

dissociative chemisorption of carbon monoxide and hydrogen.

REFERENCES

1. Bell, A. T., *Catal. Rev.* **23,** 203 (1981).
2. Bartholomew, C. H., Agrawal, P. K., and Katzer, J. R., "Advances in Catalysis," Vol. 31, p. 135. Academic Press, New York, 1982.
3. Sebastian, J. J., *Carnegie Inst. Technol. Coal Res. Lab. Contrib.*, Report No. 35 (1936).
4. King, J. G., *Trans. Inst. Gas Eng.* **88,** 218 (1938–39).
5. Naumann, A. W., *J. Catal.* **63,** 438 (1980).
6. Murchison, C. B., *in* "Proceedings, 4th International Conference on Chemistry and Uses of Molybdenum" (H. F. Barry and P. C. H. Mitchell, Eds.), Climax Molybdenum Co., Ann Arbor Science Pub., Ann Arbor, Mich., 1982.
7. Saito, M., and Anderson, R. B., *J. Catal.* **63,** 438 (1980).
8. Saito, M., and Anderson, R. B., *J. Catal.* **67,** 296 (1981).
9. Hou, P., and Wise, H., *J. Catal.* **80,** 280 (1983).
10. Wentrcek, P. R., McCarty, J. G., Ablow, C. M., and Wise, H., *J. Catal.* **61,** 223 (1980).
11. Wivel, C., Candia, R., Clausen, B. S., Morup, S., and Topsøe, H., *J. Catal.* **68,** 453 (1981).
12. Massoth, F. E., *J. Catal.* **36,** 164 (1975).
13. Schrader, G. L., and Cheng, C. P., *J. Catal.* **80,** 369 (1983).
14. Aoshima, A., and Wise, H., *J. Catal.* **34,** 145 (1974).